Journal of Pharmaceutical and Biomedical Analysis 54 (2011) 331–336

Contents lists available at ScienceDirect

Journal of Pharmaceutical and Biomedical Analysis

journal homepage: www.elsevier.com/locate/jpba

LC–MS/MS and density functional theory study of copper(II) and nickel(II) chelating complexes of elesclomol (a novel anticancer agent)

Lianming Wu*, Leon Zhou, David Q. Liu, Frederick G. Vogt, Alireza S. Kord

Analytical Sciences, GlaxoSmithKline, 709 Swedeland Road, King of Prussia, PA 19406, USA

ARTICLE INFO

Article history:
Received 15 July 2010
Accepted 7 September 2010
Available online 15 September 2010

Keywords:
Cu(II)-chelating complex of elesclomol
Irving–Williams series of bindings
Electron transfer and Cu(II) to Cu(I) reduction
LC–MS/MS
Density functional theory calculations

ABSTRACT

Elesclomol (*N*-malonyl-bis(*N*′-methyl-*N*′-thiobenzoylhydrazide)), which is a novel anticancer agent, can form chelating complexes with Fe(II), Co(II), Ni(II), Cu(II), and Zn(II) in the gas phase during electrospray ionization (ESI) mass spectrometry. In the solution phase with acidic medium during chromatographic separation, however, only Cu(II) and Ni(II) to a lesser degree favor the formation of chelating complexes with elesclomol. The Cu(II)-chelating complex $[Cu(II)+elesclomol-H]^{+\bullet}$ exhibits more complicated MS/MS fragmentation pathways than the Ni(II)-chelating complex $[Ni(II)+elesclomol-H]^{+}$. One significant difference is the ready occurrence of the electron transfer upon collision-induced dissociation (CID) of $[Cu(II)+elesclomol-H]^{+\bullet}$. This leads to the reduction of Cu(II) to Cu(I). However, such phenomenon was not observed upon CID of $[Ni(II)+elesclomol-H]^{+}$. On the basis of the density functional theory (DFT) calculations at the B3LYP/6-31+G(d)/LANL2DZ level, the Cu(II)- and Ni(II)-chelating complexes of elesclomol exist in the keto-form with tetra-coordinated trapezoid geometry in the gas phase but at different levels of distortion. As compared to the Ni(II)–elesclomol complex, the Cu(II)–elesclomol complex is more stable (by −55.25 kcal/mol). This relative stability of the chelating complexes of elesclomol is consistent with the Irving–Williams series of bindings to ligands.

1. Introduction

The transition metal ions, which inevitably exist as metal complexes in biological systems by interaction with numerous molecules capable of complexation or chelation, play an important role in the development of pharmaceutical compounds [1–3]. Elesclomol (*N*-malonyl-bis(*N*′-methyl-*N*′-thiobenzoylhydrazide), Fig. 1), which is an investigational first-in-class oxidative stress inducer that triggers apoptosis (programmed cell death) in cancer cells [4], exhibits a strong chelating affinity with the Cu(II) metal ion. The Cu(II)–elesclomol chelate can survive chromatographic separation and was detected as a distinct chromatographic peak that elutes after the peak of elesclomol. Even at the presence of trace levels of Cu(II) (i.e. 10^{-7} M in the mobile phases), the Cu(II)–elesclomol chelate could be detected at about 1% by the UV peak areas [5].

In this study, the chelating behaviors of elesclomol with Cu(II) and other first-row divalent transition metals including Fe(II), Co(II), Ni(II) and Zn(II) were examined. The investigation covers the chelating ability of the metal ions with elesclomol in the solution state during chromatographic separation and in the gas phase in the atmospheric pressure ion source of a mass spectrometer. Tandem mass spectrometry (MS/MS) was utilized to probe the difference in chelating properties of Cu(II)– and Ni(II)–elesclomol complexes. Moreover, the density functional theory (DFT) calculations were performed to obtain the optimized chelating structures to further refine the understanding of the experimental data.

2. Experimental

2.1. Chemicals

An authentic sample of elesclomol was obtained from Synta Pharmaceuticals Corporation (Lexington, MA, USA). The salts of $Fe(II)Cl_2$, $Co(II)Cl_2$, $Ni(II)Cl_2$, $Cu(II)Cl_2$ and $Zn(II)Cl_2$ were purchased from Sigma–Aldrich (St. Louis, MO, USA). A solution of 0.01 mg/mL sodium formate was supplied by Waters Corporation (Mildford, MA, USA). The HPLC-grade solvents including water and acetonitrile were purchased from Burdick and Jackson (Morristown, NJ, USA).

2.2. Liquid chromatography–mass spectrometry

Liquid chromatography–mass spectrometry (LC–MS) experiments were performed on an Agilent 1100 LC system (Agilent Technologies, Wilmington, DE, USA) coupled to a Waters Q-TOF Premier quadrupole orthogonal acceleration time-of-flight

* Corresponding author. Tel.: +1 610 270 4936; fax: +1 610 270 6608.
E-mail address: lianming.2.wu@gsk.com (L. Wu).

0731-7085/$ – see front matter © 2010 Elsevier B.V. All rights reserved.
doi:10.1016/j.jpba.2010.09.007

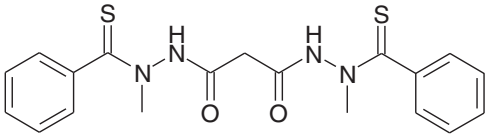

Fig. 1. Chemical structure of elesclomol, *N*-malonyl-bis(*N*′-methyl-*N*′-thiobenzoylhydrazide) ($C_{19}H_{20}N_4O_2S_2$).

mass spectrometer with LockSpray™ controlled by MassLynx 4.1 (Waters Corporation, Manchester, UK). Chromatographic separation was achieved on a Zorbax SB C18 (150 mm × 4.6 mm, 5 μm) column (Agilent Technologies, Wilmington, DE, USA) with a flow rate of 2 mL/min of mobile phase A of 0.01% trifluoroacetic acid (TFA) in water and mobile phase B of 0.01% TFA in acetonitrile. When performing the hydrogen/deuterium (H/D) exchange experiments, 0.01% TFA in deuterated water (D_2O) was used replacing mobile phase A. The HPLC gradient was initially kept at 12% B for 10 min then ramped linearly to 70% B in 20 min followed by a second gradient to 90% B in 5 min. For Q-TOF the electrospray ionization (ESI) source was operated in the positive ion mode under the following conditions: spray voltage, −3.5 kV; source and desolvation gas temperatures, 120 °C and 300 °C, respectively; argon collision gas flow rate, 0.45 mL/min in the T-Wave™ guide Mark II collision cell; collision energies, 23, 20 and 6 eV for the collision-induced dissociation (CID) of the Cu(II)-, Ni(II)-chelating complexes and protonated molecule of elesclomol, respectively; desolvation gas flow rate, 600 L/hour; sample cone voltage, 30 V. The Q-TOF instrument was calibrated with a sodium formate solution at 0.01 mg/mL. The accurate masses were measured using the internal reference ion of *m*/*z* 556.2771 (protonated leucine-enkephalin) introduced via the Lockspray™.

2.3. Theoretical calculations

The DFT calculations were performed using Gaussian 03 program [6]. Standard orientations for the Cu(II) and Ni(II) chelating complexes were generated by building the structures in Gaussview 4.1; these coordinates were then utilized for geometry optimization of the structures. Geometry optimizations were performed using Becke's three-parameter hybrid functional B3LYP [7] with the 6-31+G(d) basis set that is applied to the C, H, N, O and S atoms in the system. The LANL2DZ basis set was used to place an effective core potential on Cu or Ni by providing a group of functions that describe the inner shell electrons of Cu or Ni [8,9]. Chemical bonds were considered to exist in a structure when interatomic distances were ≤2.4 Å. The spin operator expectation values (S^2) were <0.76, indicating negligible contamination by higher spin states. The calculated structures were characterized as local energy minima by frequency analyses.

3. Results and discussion

3.1. Formation of transition metal-chelating complexes of elesclomol

The results regarding the chelating behaviors of the common first-row divalent transition metal ions are summarized in Table 1. It was found that all these metal ions (when doped in the aqueous mobile phase) can form chelating complexes with elesclomol in the ion source during ESI mass spectrometry. The formed complex ions were confirmed by the isotope fitting consistency and accurate mass measurements with an error less than 3.6 ppm. Under the acidic chromatographic separation conditions, however, only Cu(II) and Ni(II) were observed to afford the stable complexes with elesclomol and the formed chelates were detected as the

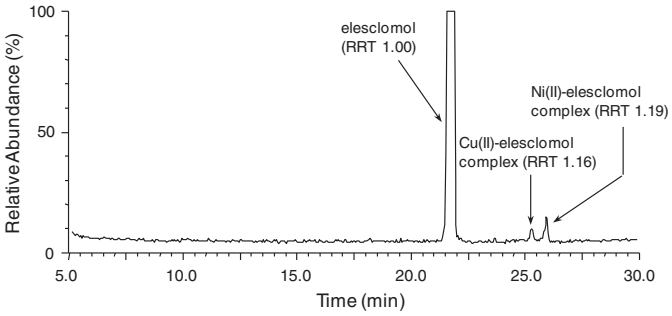

Fig. 2. Total ion current (in percent abundance with a three-time enlargement) detected by LC–MS with 10^{-5} M $NiCl_2$ doped in the aqueous mobile phase.

distinct chromatographic peaks eluting at the relative retention times (RRTs) of 1.16 and 1.19, respectively. Cu(II) shows a much higher chelating affinity with elesclomol than Ni(II). At the presence of both Cu(II)Cl_2 and Ni(II)Cl_2 (10^{-5} M each), elesclomol was completely converted into its Cu(II)-chelating complex; but no chromatographic peak corresponding to the Ni(II)-chelating complex was detected. Conversely, only a small fraction of elesclomol was converted into its Ni(II)-chelating complex at the presence of Ni(II)Cl_2 (10^{-5} M) alone. Fig. 2 displays the total ion chromatogram (TIC) from the LC–MS detection of Cu(II)- and Ni(II)-chelating complexes of elesclomol, by doping 10^{-5} M Ni(II)Cl_2 in the aqueous mobile phase to enhance the formation of the Ni(II)–elesclomol chelate for further MS/MS analysis.

3.2. Rationale for the relative stability of the Cu(II)– and Ni(II)–elesclomol complexes

Based on the Irving–Williams series of bindings to (virtually all) ligands, the binding order of the investigational metal ions is expected as Fe < Co < Ni < Cu > Zn, where the gradient in the series increase in the order of ligands O-donors < N-donors < RS^- donors < S^{2-} donors [10,11]. As described previously, the observed relative chelating affinities of these metal ions with elesclomol are in excellent agreement with the Irving–Williams series of bindings. Fig. 3 illustrates the DFT-calculated structures of Cu(II)- and Ni(II)-chelating complexes of elesclomol, suggesting that both complexes prefer the tetra-coordinated trapezoid planar geometry (distorting from the square planar geometry). Although these two complexes might experience keto–enol tautomerism in the solution phase, the DFT calculations reveal that they exist in the more stable 'keto-form' rather than the 'enol-form' structures in the gas-phase. This is supported by the H/D exchange, displaying no exchangeable proton in the complexes except the charge (proton). However, the calculated coordination bond lengths of Cu(II) to N1/N2 and S1/S2 in elesclomol are 0.08 Å and 0.11 Å longer than those of Ni(II). The longer bond lengths allow better geometry optimization by reducing intra-molecular repulsion/expansion forces and hence enhance the stability of the Cu(II)-chelating complex. The DFT calculations also indicate that Cu(II) has a stronger binding energy than Ni(II), showing that the Cu(II)–elesclomol complex is by −55.25 kcal/mol more stable than the Ni(II)–elesclomol complex.

3.3. Tandem mass spectrometry of the Cu(II)– and Ni(II)–elesclomol complexes

In order to unambiguously assign the fragment ions resulting from MS/MS of the Cu(II)- or Ni(II)-chelating complex of elesclomol, the precursor ions associated with $^{63}Cu(II)/^{65}Cu(II)$ or $^{58}Ni(II)/^{60}Ni(II)$ were individually selected and subjected to CID.

Table 1
Summary of the detection of the transition metal chelating complexes with elesclomol.[a]

Formation of metal chelating complex	Transition metal doped in the mobile phase				
	Fe(II)	Co(II)	Ni(II)	Cu(II)	Zn(II)
In the gas-phase (during ESI)	Detected as *m/z* 453/455 at RRT 1.00[b]	Detected as *m/z* 458 at RRT 1.00[b]	Detected as *m/z* 457/459 at RRT 1.00[b]	Detected as *m/z* 462/464 at RRT 1.00[b]	Detected as *m/z* 463/465 at RRT 1.00[b]
In the solution-phase (during chromatographic separation)	Not detected	Not detected	Detected as *m/z* 457/459 at RRT 1.19[b]	Detected as *m/z* 462/464 at RRT 1.16[b]	Not detected

[a] All MS detection as singly-charged complex ions.
[b] RRT is relative retention time (RRT) based on the retention time of elesclomol.

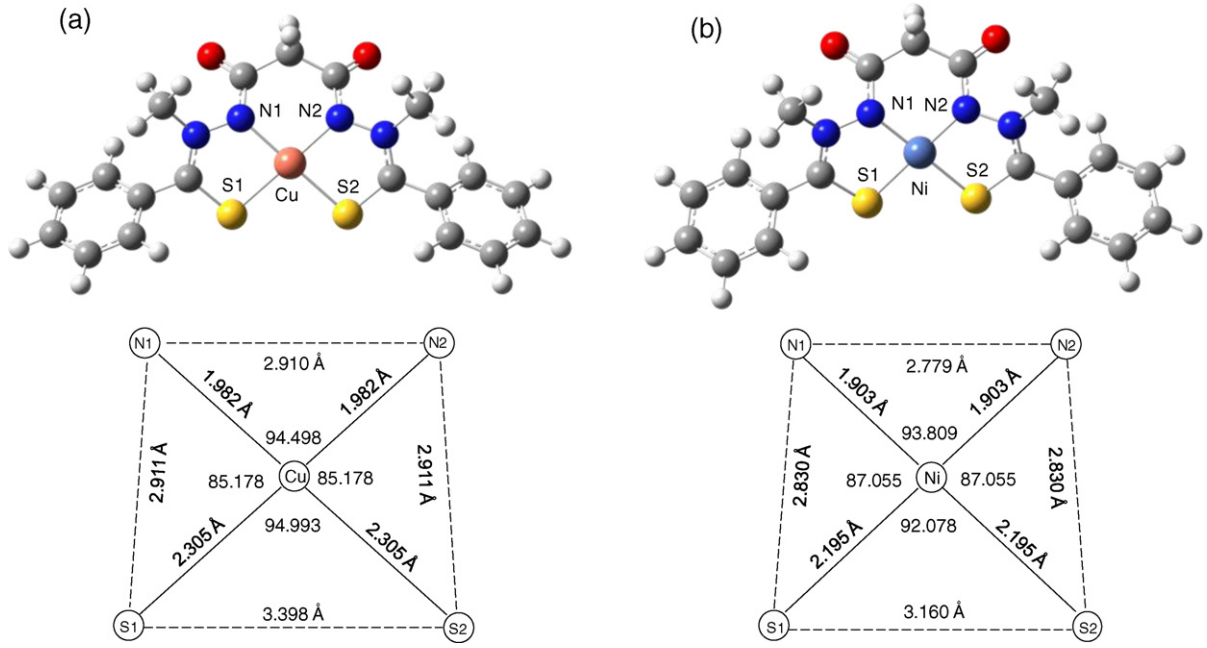

Fig. 3. Calculated structures of (a) Cu(II)- and (b) Ni(II)-chelating complexes with elesclomol.

Fig. 4a and b show the MS/MS spectra of ^{63}Cu(II)- and ^{65}Cu(II)-chelating complexes of elesclomol that are formed during the chromatographic separation. From the comparison, one can see that the peaks at *m/z* 118, 201, 217, 333, and 349 appear in the MS/MS spectra of both Fig. 4a and b, corroborating that these fragment ions do not carry either Cu(II) or Cu(I). In contrast, all other major fragment ions should contain Cu since they all show a mass difference of 2 Da due to the ^{63}Cu and ^{65}Cu isotope contributions (Table 2). As for the Cu(II)-chelating complex that is generated in the ESI source (when the aqueous mobile phase was doped with $CuCl_2$ at 10^{-7} M), MS/MS (spectrum not shown) exhibits the same fragmentation pathways. Although the coordination properties of a chelating complex may vary in the gas phase and the condensed state [12], these MS/MS data imply that the Cu(II)-chelating complexes produced in the ESI source and in the solution should have the same conformation in the gas phase; otherwise they would give different MS/MS spectra [13]. Similarly, the Ni(II)-chelating complexes that is generated in solution during the chromatographic separation (Fig. 5) and in the ESI source (spectrum not shown) show the same fragmentation pathways, suggesting that they also have the same conformation in the gas phase. However, by comparison with the fragmentation of the Cu(II)-chelating complex with elesclomol, the MS/MS spectra of the Ni(II)–elesclomol chelate is much simpler, giving rise to three major fragment ions which are summarized in Table 3. This is consistent with the DFT calculations showing the relative binding energies of Cu(II) > Ni(II) with elesclomol.

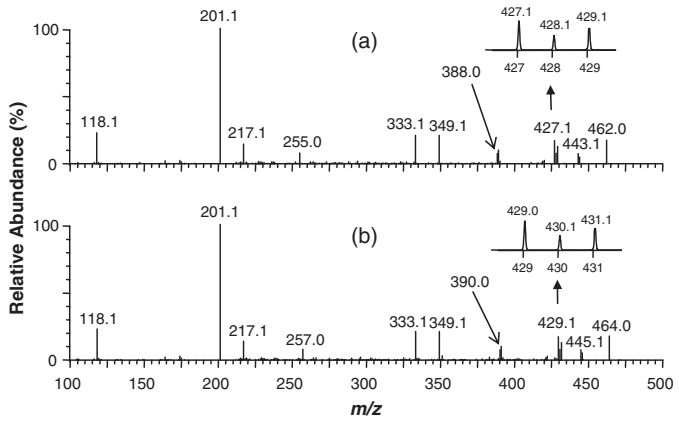

Fig. 4. MS/MS spectra of (a) the ^{63}Cu(II)- and (b) ^{65}Cu(II)-chelating complexes with elesclomol. Note that the insets are the enlarged portions of the peak envelops at (a) *m/z* 427–429 and (b) *m/z* 429–431.

There is one common fragment ion of *m/z* 118 that results from CID of both Cu(II)- and Ni(II)-chelating complexes of elesclomol and this ion was not observed in the MS/MS spectrum of the protonated molecule ($[M+H]^+$) of elesclomol (Fig. 6). When ^{13}C-labeled (at two phenyl rings) elesclomol was used, the *m/z* becomes 124, corroborating that one phenyl ring is remained in this fragment ion.

Table 2
Summary of the MS/MS fragmentation of [Cu(II)+elesclomol−H]$^+$.

m/z of fragment ion	With Cu	Cu(II) to Cu(I) reduction	Main fragmentation mechanism	Fragment ion assignment[a]	Fragment ion observed in MS/MS of [M+H]$^+$
118	No	Not applicable	Rearrangement (Scheme 1)	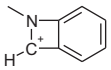	No
201	No	Not applicable	Proton transfer followed by rearrangement	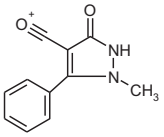	Yes
217	No	Not applicable	Proton transfer followed by rearrangement	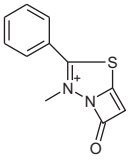	Yes
^{63}Cu: 255 ^{65}Cu: 257	Yes	Yes	Cleavage via loss of 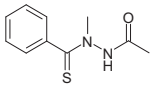 associated with Cu(II) to Cu(I) reduction	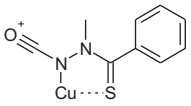	Not applicable
333	No	Not applicable	Proton transfer followed by rearrangement	Loss of two H_2S from [M+H]$^+$	No (but loss of one H_2S)
349	No	Not applicable	Proton transfer followed by rearrangement	Loss of ($H_2O + H_2S$) from [M+H]$^+$	No (but loss of one H_2O)
^{63}Cu: 388, 389 ^{65}Cu: 390, 391	Yes	Yes	Cleavage via loss of  with further Cu(II) to Cu(I) reduction[b]	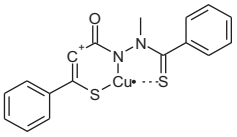	Not applicable
^{63}Cu: 427, 428, 429 ^{65}Cu: 429, 430, 431	Yes	Yes	Rearrangement via loss of H_2S with further loss of H$^\bullet$ radical and Cu(II) to Cu(I) reduction[b]	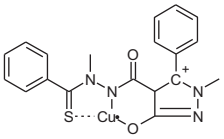	Not applicable
^{63}Cu: 443, 444 ^{65}Cu: 445, 446	Yes	No	Rearrangement via loss of H_2O with further loss of H$^\bullet$ radical[b]	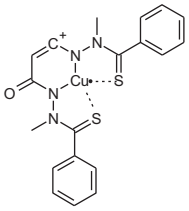	Not applicable

[a] The elemental compositions of fragment ion assignments were confirmed by the accurate mass measurements within an error of 4.5 ppm.
[b] The proposed structures of the fragment ions of (1) *m/z* 427/429 & 443/445 (via the further H$^\bullet$ radical loss) and (2) *m/z* 389/391 & 429/431 (via the Cu(II) to Cu(I) reduction) are not shown.

From these experimental evidences it is believed that both complex ions, [Cu(II)+elesclomol−H]$^{+\bullet}$ and [Ni(II)+elesclomol−H]$^+$, could undergo a rearrangement via the ring formation and simple bond cleavage to give rise to the ion of *m/z* 118 (Scheme 1).

3.4. Electron transfer upon CID of the Cu(II)–elesclomol complex

Regarding the Cu-containing fragment ions of *m/z* (255/257), (388/390 and 389/391), (427/429, 428/430 and 429/431) and (443/445 and 444/446), each pair of *m/z* corresponds to the ^{63}Cu(II) and ^{65}Cu(II) isotope contributions. Besides the common fragmentation pathways via rearrangements and cleavages upon CID of [Cu(II)+elesclomol−H]$^{+\bullet}$, the further loss of H$^\bullet$ radical (yielding the ions of *m/z* 427/429 and 443/445) and the reduction of Cu(II) to Cu(I) via the electron transfer (giving rise to the ions of *m/z* 255/257, 389/391 and 429/431) were observed. These observations are consistent with the gas-phase dissociation behavior of other Cu(II)-chelating complexes including the chelates of histidine [14], fatty acids [15] and lactic acid [16]. In contrary, the reduction of Ni(II) to Ni(I) does not occur upon CID of [Ni(II)+elesclomol−H]$^+$ (Table 2). The ready occurrence of the electron transfer and the H$^\bullet$ radical loss is probably due to fragmentation of the radical cation

Table 3
Summary of the MS/MS fragmentation of [Ni(II)+elesclomol−H]$^+$.

m/z of fragment ion	With Ni	Ni(II) to Ni(I) reduction	Main fragmentation mechanism	Fragment ion assignment[a]	Fragment ion observed in MS/MS of [M+H]$^+$
118	No	Not applicable	Rearrangement (Scheme 1)	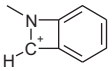	No
^{58}Ni: 389 ^{60}Ni: 391	Yes	No	Rearrangement	Loss of two H_2S	Not applicable
^{58}Ni: 442 ^{60}Ni: 444	Yes	No	Simple cleavage	Direct loss of $^{\bullet}CH_3$ radical	Not applicable

[a] The elemental compositions of fragment ion assignments were confirmed by the accurate mass measurements within an error of 3.8 ppm.

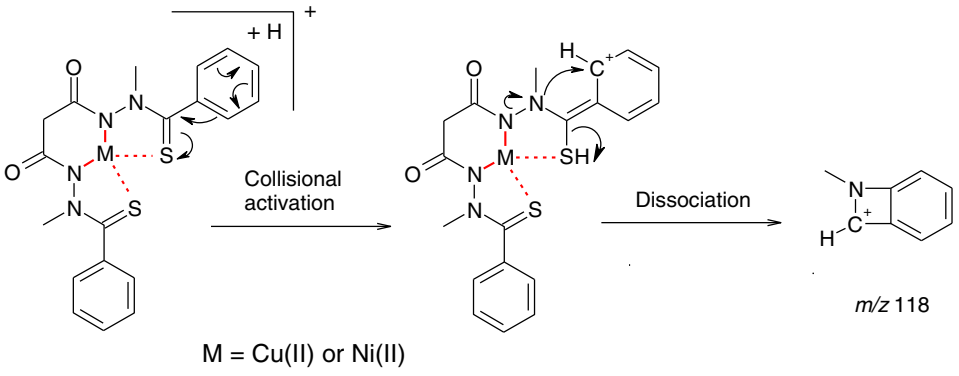

Scheme 1. The formation of the product ion of *m/z* 118 via the rearrangement of Cu(II)- and Ni(II)-chelating complexes of elesclomol upon CID. Note that the radical in [Cu(II)+elesclomol−H]$^{+\bullet}$ is not shown for drawing simplicity.

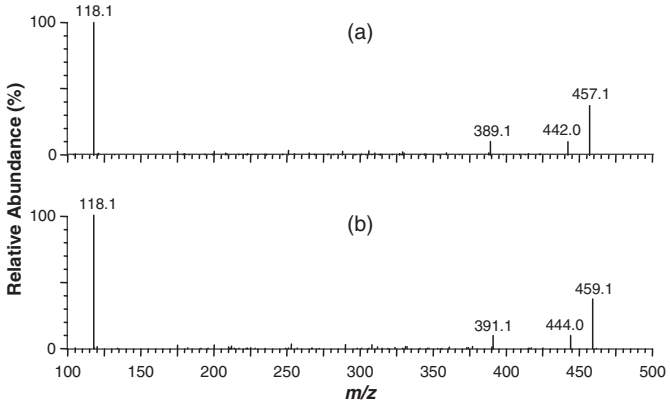

Fig. 5. MS/MS spectra of (a) the ^{58}Ni(II)- and (b) ^{60}Ni(II)-chelating complexes with elesclomol.

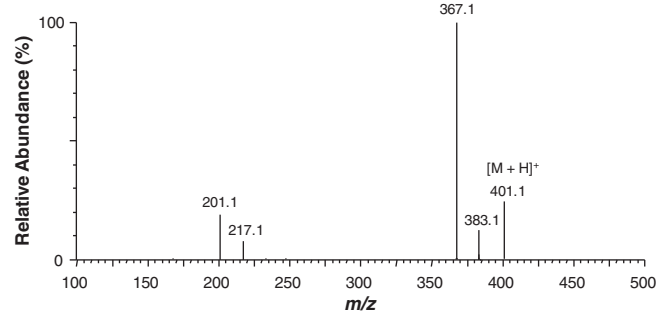

Fig. 6. MS/MS spectrum of the protonated molecule of elesclomol at *m/z* 401.

of the Cu(II)–elesclomol complex (open-shell species) in the gas phase that results from the d^9 electronic configuration of Cu(II).

4. Conclusions

Elesclomol can form chelating complexes with Fe(II), Co(II), Ni(II), Cu(II) and Zn(II) in the gas phase during ESI mass spectrometry. In the solution phase, however, only Cu(II) and Ni(II) but less significantly favor the formation of the chelating complexes with elesclomol. The Cu(II)-chelating complex exhibits more complicated MS/MS fragmentation pathways than the Ni(II)-chelating complex, owing to the strong binding with elesclomol and the ready occurrence of the electron transfer upon collisional activation. Such phenomenon was not observed upon CID of the Ni(II)-chelating complex. Based on the DFT calculations, the Cu(II)- and Ni(II)-chelating complexes of elesclomol exist in the keto-form with tetra-coordinated trapezoid geometry in the gas-phase but the Cu(II)-chelating complex exhibits longer coordination bond lengths for better geometry optimization. As compared to Ni(II) and other metal ions, Cu(II) shows an unusually higher chelating affinity with elesclomol and this observation is consistent with the Irving–Williams series of bindings of metal ions. This study provides insights into the intrinsic chelating properties of Cu(II)–elesclomol complex and is useful for pursuing analytical applications in pharmaceutical industry (e.g. pharmaceutical manufacturing equipment cleaning verification) by developing a sensitive and selective method for detection and quantitation of elesclomol utilizing reactive desorption electrospray ionization (DESI) [17–20] with a Cu(II)-containing spray solution.

Acknowledgments

The authors would like to thank Drs. Christopher Brook, Joe Sisko and Mr. Paul MacGregor (GlaxoSmithKline) for the helpful discus-

sion and contributions. The authors also want to acknowledge Dr. Jianhua Shen (Synta Pharmaceuticals) for his contributions to the idea of elesclomol chelating with Cu(II) and Ni(II), the method of liquid chromatographic separation and the authentic sample of elesclomol.

References

[1] D. Cen, D. Brayton, B. Shahandeh, F.L. Meyskens Jr., P.J. Farmer, J. Med. Chem. 47 (2004) 6914–6920.
[2] D.S. Kalinowski, P.C. Sharpe, P.V. Bernhardt, D.R. Richardson, J. Med. Chem. 50 (2007) 6212–6225.
[3] D. Jiang, L. Men, J. Wang, Y. Zhang, S. Chickenyen, Y. Wang, F. Zhou, Biochemistry 46 (2007) 9270–9282.
[4] J.R. Kirshner, S. He, V. Balasubramanyam, J. Kepros, C.Y. Yang, M. Zhang, Z. Du, J. Barsoum, J. Bertin, Mol. Cancer Ther. 7 (2008) 2319–2327.
[5] S. Yang, A. Caltabiano, L. Wu, J. Shen, J. Chen, A.S. Kord, L. Zhou, J. Pharm. Biomed. Anal. 53 (2010) 371–375.
[6] M.J. Frisch, G.W. Trucks, H.B. Schlegel, G.E. Scuseria, M.A. Robb, J.R. Cheeseman, V.G. Zakrzewski, J.A. Montgomery, R.E. Stratmann, J.C. Burant, S. Dapprich, J.M. Millam, A.D. Daniels, K.N. Kudin, M.C. Strain, O. Farkas, J. Tomasi, V. Barone, M. Cossi, R. Cammi, B. Mennucci, C. Pomelli, C. Adamo, S. Clifford, J. Ochterski, G.A. Petersson, P.Y. Ayala, Q. Cui, K. Morokuma, D.K. Malick, A.D. Rabuck, K. Raghavachari, J.B. Foresman, J. Cioslowski, J.V. Ortiz, A.G. Baboul, B.B. Stefanov, G. Liu, A. Liashenko, P. Piskorz, I. Komaromi, R. Gomperts, R.L. Martin, D.J. Fox, T. Keith, M.A. Al-Laham, C.Y. Peng, A. Nanayakkara, C. Gonzalez, M. Challacombe, P.M.W. Gill, B. Johnson, W. Chen, M.W. Wong, J.L. Andres, C. Gonzalez, H.-M. Gordon, E.S. Replogle, J.A. Pople, Gaussian 03, Revision D.02, Gaussian, Inc., Pittsburgh, PA, 2003.
[7] R.G. Parr, W. Yang, Ann. Rev. Phys. Chem. 46 (1995) 701–728.
[8] P.J. Hay, W.R. Wadt, J. Chem. Phys. 82 (1985) 299–310.
[9] P.J. Hay, W.R. Wadt, J. Chem. Phys. 82 (1985) 270–283.
[10] H.M. Irving, R.J.P. Williams, J. Chem. Soc. (1953) 3192–3210.
[11] R.J.P. Williams, J. Inorg. Biochem. 88 (2002) 241–250.
[12] J.R. Hartman, R.W. Vachet, W. Pearson, R.J. Wheat, J.H. Callahan, Inorg. Chim. Acta 343 (2003) 119–132.
[13] W.A. Tao, D. Zhang, E.N. Nikolaev, R.G. Cooks, J. Am. Chem. Soc. 122 (2000) 10598–10609.
[14] T. Song, C.N.W. Lam, D.C.M. Ng, G. Orlova, J. Laskin, D.-C. Fang, I.K. Chu, J. Am. Soc. Mass Spectrom. 20 (2009) 972–984.
[15] C. Afonso, A. Riu, Y. Xu, F. Fournier, J.-C. Tabet, J. Mass Spectrom. 40 (2005) 342–349.
[16] M.R. Kumar, S. Prabhakar, M.K. Kumar, T.J. Reddy, M. Vairamani, Rapid Commun. Mass Spectrom. 19 (2005) 113–120.
[17] Z. Takats, J.M. Wiseman, B. Gologan, R.G. Cooks, Science 306 (2004) 471–473.
[18] D.R. Ifa, C. Wu, Z. Ouyang, R.G. Cooks, Analyst 135 (2010) 669–681.
[19] Z. Miao, H. Chen, J. Am. Soc. Mass Spectrom. 20 (2009) 10–19.
[20] Y. Zhang, H. Chen, Int. J. Mass Spectrom. 289 (2010) 98–107.